Available online at www.sciencedirect.com
ScienceDirect
Journal of Magnetism and Magnetic Materials 311 (2007) 347–353
www.elsevier.com/locate/jmmm

Field-induced motion of ferrofluids through immiscible viscous media: Testbed for restorative treatment of retinal detachment

Olin T. Mefford[a], Robert C. Woodward[b], Jonathan D. Goff[a], T.P. Vadala[a], Tim G. St. Pierre[b], James P. Dailey[c], Judy S. Riffle[a,*]

[a]*Macromolecules and Interfaces Institute, Virginia Tech, Blacksburg, VA 24061, USA*
[b]*School of Physics, The University of Western Australia, Crawley, WA 6009, Australia*
[c]*NanoMedics LLC, Erie, PA 15607, USA*

Available online 18 December 2006

Abstract

Biocompatible, hydrophobic ferrofluids comprised of magnetite nanoparticles dispersed in polydimethylsiloxane show promise as materials for the treatment of retinal detachment. This paper focuses on the motion of hydrophobic ferrofluid droplets traveling through viscous aqueous media, whereby the movement is induced by gradients in external fields generated by small permanent magnets. A numerical method was utilized to predict the force on a spherical droplet, and then the calculated force was used to estimate the time required for the droplet to reach the permanent magnet. The calculated forces and travel times were verified experimentally.

Keywords: Ferrofluid; Magnetite; Polydimethylsiloxane; Retina; Ferrohydrodynamics; Nanoparticle; Retinal detachment

1. Introduction

We worked for several years to develop biocompatible polysiloxane ferrofluids for treating retinal detachments [1–5]. Retinal detachment is a leading cause of blindness, and currently available treatments fail in as many as 1/3 of complicated retinal detachment patients, resulting in partial or complete loss of vision for several million people worldwide. A retinal tear provides a pathway for vitreous fluid to pass through and underneath the retina, thus detaching the retina from the choroid. The goal of surgery is to close any holes in the retina, preventing further fluid flow into the subretinal space, allowing for reattachment of the retina.

The proposed treatment (Fig. 1) requires synthesizing magnetic nanoparticles and complexing them with a functionalized polysiloxane, then dispersing the complex in a non-functional polysiloxane oligomer to form the ferrofluid. The fluid can be injected through a fine needle into the vitreous cavity of the eye in apposition to a tiny permanent magnet inserted beneath Tenon's capsule on the outside of the scleral wall of the eye. The polysiloxane fluid is hydrophobic and has a high interfacial tension against the vitreous gel, and thus a stable spherical ferrofluid droplet forms within the aqueous environment. The permanent magnet attracts the ferrofluid droplet toward the side of the eye, and it is anticipated that the droplet can then seal a retinal hole.

Understanding the motion of a ferrofluid droplet as it travels in the eye is important for the success of this procedure. The permanent magnet on the exterior of the eye should generate a magnetic field of sufficient strength to pull the ferrofluid droplet to the retinal tear in a reasonable amount of time. The droplet volume must also be considered, as it will likely affect the size of the hole that can be sealed, as well as the overall motion of the droplet. Mathematical models for the motion of ferrofluids were described by Shliomis [6–11] and Felderhof [12–14]. Others investigated the use of gradient fields for positioning ferrofluids in microfluidic [15], capillary [16], and controlled rheological systems [17–19]. Rinaldi et al. [20] published an excellent review on this subject.

The intention of this research was to demonstrate the control of polysiloxane ferrofluid motion through a viscous

*Corresponding author. Tel.: +1 540 231 8214; fax: +1 540 231 8517.
E-mail address: judyriffle@aol.com (J.S. Riffle).

0304-8853/$ - see front matter © 2006 Elsevier B.V. All rights reserved.
doi:10.1016/j.jmmm.2006.10.1174

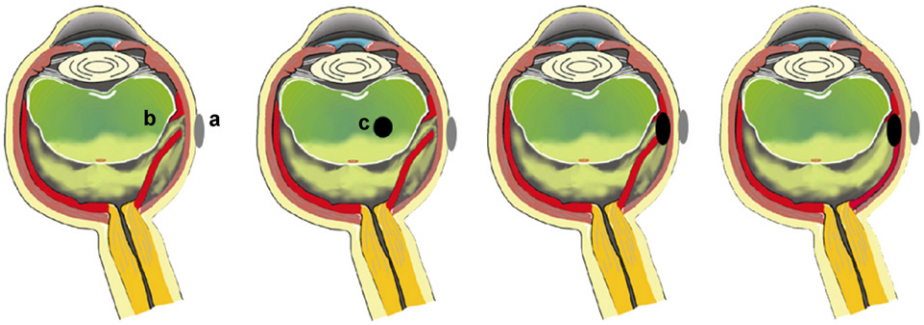

Fig. 1. Proposed procedure for treating a retinal detachment: (1) A permanent magnet (a) with a pre-aligned magnetic field is placed in the conjunctiva proximal to the site of the retinal detachment (b), (2) a ferrofluid droplet (c) is injected into the vitreous humor, (3) attracted to the permanent magnet, the ferrofluid closes the hole in the retina, and (4) the body absorbs the liquid that has accumulated underneath the retina.

aqueous medium. Fundamental magnetic properties of the ferrofluid, mathematical calculations of the forces applied to ferrofluid droplets by an external permanent magnet, and simulations of the mobility of a ferrofluid droplet as it travels through the medium will be described.

2. Experimental

2.1. Materials

Hexamethylcyclotrisiloxane (D_3, Gelest) was dried over calcium hydride and sublimed under vacuum into pre-weighed, flame dried, roundbottom flasks, each containing a magnetic stirring bar. The flasks were purged with argon and re-weighed to determine the amount of D_3 in each flask. Cyclohexane (EM Science, 99%) was stirred with concentrated sulfuric acid for 1 week, washed with deionized water until neutral, stirred over calcium hydride, distilled, stored over sodium under a nitrogen atmosphere, and distilled before use. Tetrahydrofuran (THF) (EM Science, 99.5%) was dried over calcium hydride, distilled, stored as the purple sodium/benzophenone dispersion under nitrogen, and distilled just before use. Toluene (Burdick and Jackson, 99.9%) was distilled from calcium hydride and deoxygenated by purging with dry nitrogen before use. Hydrochloric acid solution was prepared by adding 5 mL of concentrated hydrochloric acid (37 wt% in water, EM Science) to 5 mL of deionized water. Ferric chloride hexahydrate ($FeCl_3 \cdot 6H_2O$) and ferrous chloride tetrahydrate ($FeCl_2 \cdot 4H_2O$), both from Aldrich, were stored under nitrogen in a desiccator and used as received. Ammonium hydroxide (Alfa Aesar, 50% v/v aqueous), mercaptoacetic acid (97%, Aldrich), 2,2′-azobisisobutyronitrile (AIBN, 98%, Aldrich), n-butyllithium (2.0 M, Aldrich), trivinylchlorosilane (Gelest), trimethylchlorosilane (Gelest), MQP-B NdFeB powder (kindly donated by Magnequench, Toronto, Canada), Provisc™ solution (Alcon Inc., generously supplied by the Lion's Eye Institute, Nedlands, WA, Australia), and Tarzan's Grip® (Selleys Pty Ltd.) general purpose clear cyanoacrylate adhesive were used as received.

2.2. Ferrofluid synthesis

The methods for synthesizing the ferrofluid components were previously reported [5]. The ferrofluid utilized in the present work was comprised of magnetite nanoparticles complexed with a carboxylate-functional polydimethylsiloxane (PDMS) (Fig. 2), and this complex was dispersed in a 5000 g mol^{-1} PDMS carrier fluid. The complex contained 50 wt% of magnetite and 50 wt% of the PDMS dispersant, and this complex was combined with the carrier fluid (50 wt% complex: 50 wt% carrier fluid), yielding a ferrofluid that contained 25 wt% magnetite. A brief synthetic procedure is described.

The PDMS dispersion stabilizer having three carboxylic acid groups at one end was prepared by first subliming D_3 (27.44 g) into a septum sealed, flame dried, roundbottom flask. The flask was purged with nitrogen, and cyclohexane (30 mL) was added via a syringe to dissolve the D_3. The *n*-butyllithium initiator (3.5 mL of a 2.5 M solution, 8.75×10^{-3} mol) was added to the reaction, and the solution was stirred at 25 °C for 1 h. THF (10 mL) was charged to the solution as a reaction promoter, and the polymerization was conducted at 25 °C. ^{1}H NMR was utilized to monitor the progress of the living anionic polymerization. The polymer was terminated by adding excess trivinylchlorosilane (2.2 mL, 0.0142 mol) at ~70–80% conversion and allowing the mixture to stir overnight. The excess trivinylchlorosilane was removed under vacuum, then the product was precipitated by pouring into methanol. The PDMS oligomer was diluted with chloroform, washed three times with deionized water, the chloroform was removed, and the polymer was dried under vacuum at 80 °C overnight. The synthetic procedure for the 5000 g mol^{-1} PDMS carrier fluid was similar to the one outlined above, except the living anionic polymerization was terminated with trimethylchlorosilane.

The thiolene addition of mercaptoacetic acid to the trivinyl-terminated PDMS oligomer was as follows. A 2500 g/mol trivinylsiloxy terminated PDMS (12.3 g, 0.0148 equiv vinyl) was added into a flame dried, roundbottom flask and dissolved in toluene (60 mL). Argon was bubbled

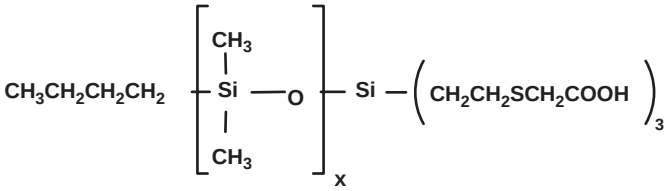

Fig. 2. Tricarboxylic acid terminated PDMS used to stabilize the magnetite nanoparticles.

through the solution for approximately 2 h to deoxygenate the reaction mixture. AIBN (0.0035 g, 0.0213 mmol) and mercaptoacetic acid (1.39 mL, 0.0200 mol) were added to the reaction vessel, and the flask was purged with argon. The reaction was heated to 80 °C and stirred for 1 h. Reaction completion was confirmed by observing the disappearance of the vinyl proton peaks at δ 5.8–6.2 ppm in the ^{1}H NMR spectrum. The solvent was removed under vacuum, and the polymer was dissolved in methanol and stirred for 30 min. Deionized water was added to the solution until the polymer coagulated. The methanol/deionized water coagulation process was repeated five times, and the polymer was dried under vacuum at 80 °C.

Synthesis of the magnetite nanoparticles and subsequent adsorption of the carboxylate-functional PDMS stabilizer onto the magnetite nanoparticle surfaces was achieved as follows. The composition was adjusted so that the final complex contained 50 wt% of magnetite and 50 wt% of the PDMS stabilizer. Magnetite nanoparticles were prepared using a chemical co-precipitation of iron salts. Iron (III) chloride hexahydrate (2.01 g, 7.44 mmol) and iron (II) chloride tetrahydrate (0.736 g, 3.70 mmol) were weighed into separate roundbottom flasks and each was dissolved in 20 mL of deoxygenated water. The two iron salt solutions were added to a 500 mL, three necked, roundbottom flask fitted with an overhead stirring apparatus and a pH electrode. Ammonium hydroxide solution (~15 mL) was added via syringe until the rapidly stirring solution turned black and reached a pH of 9–10. The PDMS dispersion stabilizer (0.9 g) was dissolved in dichloromethane (20 mL) and the solution was added to the basic, aqueous, magnetite dispersion. After stirring for 30 min, aqueous HCl (~18.5 wt% HCl in water) was added slowly until the solution became slightly acidic (~6 mL was required to reach pH 5–6). The heterogeneous dispersion was stirred for 1 h, and then the dichloromethane was removed under vacuum. The magnetite complex was collected with a magnet and the water was decanted. The PDMS–magnetite complex was washed five times with water, five times with methanol, then dried overnight at 40 °C under reduced pressure.

To prepare the ferrofluid, a 5000 g/mol PDMS oligomer having trimethylsilyl endgroups (2 g) and the PDMS stabilizer–magnetite complex (2 g, 50 wt% PDMS and 50 wt% magnetite) were added to a scintillation vial. Chloroform (20 mL) was added to the vial. Once the carrier fluid and complex were dissolved, the dispersion was sonicated with a Biologics ultrasonic homogenizer (model 150V/T) for 15 min using the full power setting on a microtip probe and a 50% pulse. After sonication, the chloroform was removed under reduced pressure, yielding a PDMS–magnetite ferrofluid.

2.3. Ferrofluid characterization

Samples of ferrofluid were sealed in pre-weighed polycarbonate sample chambers and placed in a Quantum Systems MPMS SQUID magnetometer. The magnetization of the ferrofluids was measured between +70,000 and −70,000 Oe at room temperature. The density of the ferrofluid was determined by weighing the mass of the fluid in a sample chamber of known volume.

2.4. Preparation and characterization of the permanent magnet

NdFeB powder was dispersed into a cyanoacrylate adhesive (80/20 wt/wt powder/adhesive), and the mixture was pressed into rectangular Teflon molds that were 5 mm deep, 5 mm wide, and 20 mm long. The samples were cured overnight at 25 °C in air. While still in the mold, the samples were placed in a 12 T field to magnetize the magnet with the field direction perpendicular to the thickness of the magnet. The magnets were removed from the molds and the fields generated by the magnets were measured with a Hall probe every 1 mm from the center of the surface of the magnet to 30 mm away along the axis of magnetization. The data was fitted with a 5th order polynomial.

2.5. Measurement of magnetic force via a load cell

The fields from an electromagnet at 1, 2, and 3 A of current were measured with a Hall probe as described for the permanent magnet. A 0.0304 g sample of ferrofluid was then placed on a top-loading electronic microbalance (Mettler Toledo AB54). A spacer was placed between the sample and the balance to ensure that the magnetic fields from the electromagnet did not affect the performance of the balance. The electromagnet was placed 5, 9, 16, and 20 mm above the ferrofluid and the weights of the ferrofluid at each distance with 0, 1, 2, or 3 A of current passing through the electromagnet were recorded. The magnetic forces (F_M) were determined by applying the acceleration due to gravity to the weight differences with and without the electromagnetic field:

$$F_M = \left(9.8\frac{m}{s^2}\right)(wt_{\text{in field}} - wt_{\text{without field}}). \quad (1)$$

2.6. Time-lapse photography of ferrofluid motion through a viscous medium

To test the accuracy of the numerical calculations, time-lapse photography was used to observe the motion of

ferrofluid droplets through a viscous medium. An experiment was devised to approximate conditions within an eye. Hollow glass spheres, with 22 mm inner diameter and 24 mm outer diameter, were charged with Provisc™ (sodium hyaluronate) solution, a "viscoelastic" commonly used in eye surgery, which has a viscosity of ~50 Pa s. Droplets of ferrofluid were introduced into the center of the glass sphere. The mass increase resulting from the ferrofluid was measured with a microbalance, and the droplet volume was calculated based on the density of the fluid assuming that the droplet was spherical. A permanent magnet was placed on the side of the sphere. Photographic images were taken every 15 s as the droplet moved from the center to the side of the glass sphere.

Theory: The magnetic force, F_M, acting on an object is given by [21]

$$F_M = \mu_0 \nabla(m \bullet H), \tag{2}$$

where m is the magnetic moment of the object, μ_0 is the magnetic permeability of free space and H is the magnetic field. A number of assumptions were made to simplify the analyses. We assumed a point dipole approximation, where the magnetization of the droplet was along the field direction and only gradients in the field direction (x direction) were considered. In this case, the magnetic force acting on a spherical droplet traveling through a uniform aqueous medium towards a permanent magnet on the exterior of the eye can be simplified to

$$F_M(x) = VM(x)\mu_0 \frac{dH}{dx}, \tag{3}$$

where V is droplet volume, M is the magnetization of the PDMS ferrofluid droplet, and dH/dx is the gradient of the magnetic field, H, with respect to distance, x, from the permanent magnet.

If the magnet is sufficiently large, then the field generated by the permanent magnet as a function of distance from its surface, $H(x)$, can be measured with a Hall probe. SQUID magnetometry was utilized to measure the magnetization of a ferrofluid as a function of the applied magnetic field ($M(H)$). By substituting $H(x)$ in $M(H)$, the magnetization of the droplet can be defined in terms of its distance from the permanent magnet, $M(x)$. The result can be utilized to calculate the force generated by the permanent magnet on the PDMS droplet as a function of its distance from the magnet.

The motion of a ferrofluid droplet through the vitreous humor will be opposed by viscous drag. If we assume that the droplet maintains a spherical shape, then the viscous drag force, F_D, on a droplet with radius, r, moving through an immiscible fluid with a velocity, U, and a viscosity, η, can be described by the generalized Stokes equation:

$$F_D = 6r\pi\eta U. \tag{4}$$

Solving for velocity yields

$$U = \frac{F_D}{6r\pi\eta}. \tag{5}$$

To calculate steady-state velocity, the magnetic force, F_M, can be equated to the drag force, F_D, from Eqs. (3) and (4) respectively, which leads to an expression for the steady-state velocity:

$$U(x) = \frac{F_M(x)}{6r\pi\eta}. \tag{6}$$

For a highly viscous medium, the time required for the droplet to accelerate to the steady-state velocity is relatively insignificant. Thus, the assumption that the droplet always moves at the steady-state velocity was invoked. Knowing the velocity, the time required for the droplet to travel from a point in the viscous medium to the permanent magnet can be estimated. Since $U(x)$ gives the velocity at a point in space, integration across the distance to be traveled, Z, results in the time required for travel to the permanent magnet,

$$\text{time} = \int_0^z \frac{1}{U(x)}\,dx = \int_0^z \frac{6r\pi\eta}{F_M(x)}\,dx. \tag{7}$$

3. Results and discussion

A series of experiments was conducted to understand the behavior of the PDMS ferrofluid in gradient magnetic fields. Magnetic moments measured by SQUID magnetometry were converted to units of magnetization by dividing by the volume of ferrofluid in the sample chamber (converting from $A\,m^2$ to A/m). The density of the ferrofluid was determined to be 1.32 g/mL. The SQUID data was fitted with a Langevin function to describe the magnetization, M, in terms of the field, H.

A permanent magnet was prepared from NdFeB powder in a polycyanoacrylate network. The moments of the NdFeB particles were aligned in a 12 T field, and the resulting magnetic field generated by the permanent magnet was mapped with a Hall probe. This data was fitted with a 5th order polynomial to mathematically describe the field, H, in terms of distance from the magnet, x (Fig. 3). The field gradient dH/dx was found by differentiating this equation. The polynomial curves from the Hall probe measurements were combined with the Langevin fit function from the SQUID measurements on the ferrofluid to yield the magnetization, $M(x)$, as a function of distance from the magnet. The resulting expression was substituted into Eq. (3) to provide a function for the force on a droplet of known volume resulting from a permanent magnet at a known distance, x, from the droplet. This expression was utilized to calculate the forces exerted on a 1 mm diameter droplet of ferrofluid (Fig. 4).

Experiments were designed to verify the calculations of forces imposed on the ferrofluids. A ferrofluid was placed on a balance and an electromagnet was positioned above the ferrofluid. When the magnetic field was applied, the mass read by the balance was reduced due to the upward

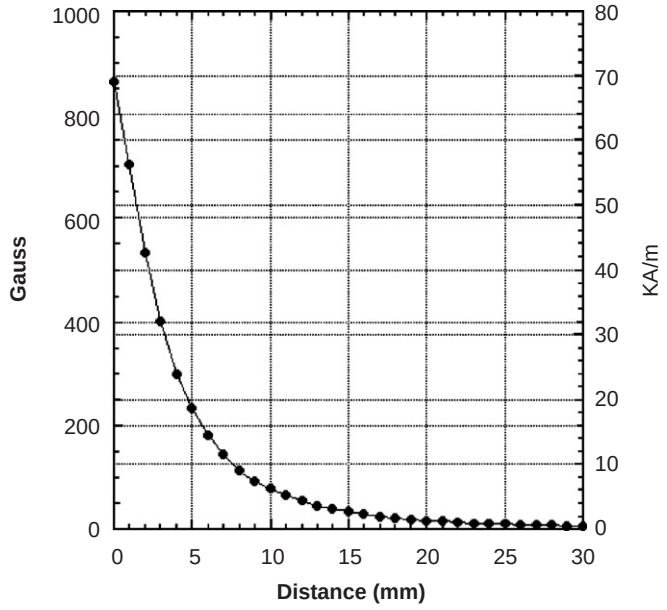

Fig. 3. Field map around a 5 mm thick by 5×20 mm bar magnet containing 80 wt% NdFeB powder.

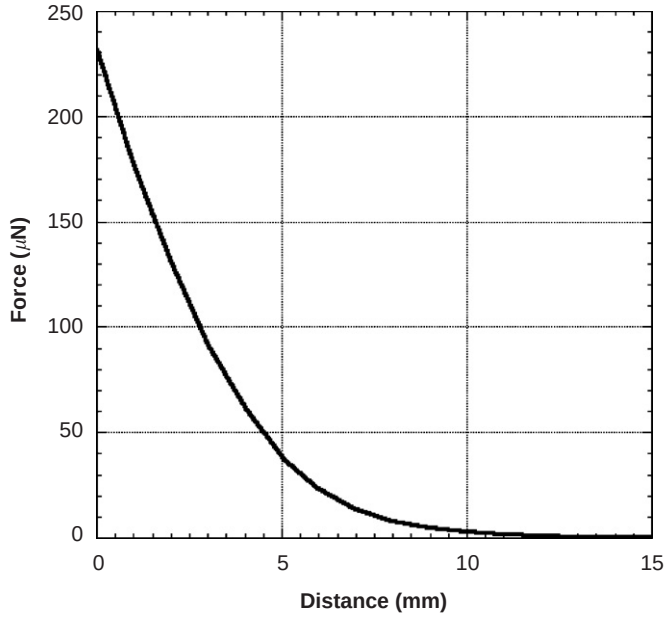

Fig. 4. Calculated force on a 1 mm diameter droplet of ferrofluid generated from a 5 mm thick by 5×20 mm bar magnet containing 80 wt% NdFeB powder with the magnetic field through the thickness.

force on the ferrofluid generated by the electromagnet. The magnetic forces were determined by subtracting the force due to gravity from the total forces. At low currents (low fields), the magnetic forces derived from the numerical method matched experimental results, but the method over-predicted the forces at higher currents (Fig. 5). Based on permanent magnets suitable for the given application to eye surgery, we anticipate that forces only up to ~200 μN will be required to attract the ferrofluid droplet to the magnet (assuming that the droplet will be introduced approximately 10 mm from the magnet and reasonable travel times are about 10 min). Thus, it was reasoned that predictions of the magnetic force imposed on these ferrofluids by an external magnet are possible using the simplified expression Eq. (3).

The amount of time required for a ferrofluid droplet to travel through a viscous medium to a permanent magnet was approximated based on the force calculations. By assuming a steady-state velocity, the drag force was equated to magnetic force, resulting in a function for the velocity at a given distance from the magnet Eq. (6). The reciprocal of the velocity function was integrated to estimate the time required for a spherical droplet to travel through the aqueous medium. Travel times were calculated for a series of droplets of varying diameters moving through an aqueous medium with a viscosity of 50 Pa s (Fig. 6). This viscosity was selected because it is similar to the viscosities of fluids used as replacements for the aqueous humor in the eye. As expected, the estimated travel times indicate that larger droplets travel faster than smaller droplets. In addition, the velocity increases as the droplet moves closer to the magnet. Based on these predictions, the position at which the droplet would be introduced into the eye in relation to the position of the permanent magnet is important. For example, if the surgeon injects a 2 mm diameter droplet of ferrofluid 12 mm away from the side of the eye, it would take approximately twice as long to travel compared to a droplet placed 10 mm away.

As a comparison to calculated travel times, an experiment was devised to simulate the environment of the eye. Glass spheres were filled with Pro-visc^{TM} aqueous solution to represent the eye. The permanent magnet was placed on the outside of the glass, and a droplet of ferrofluid was injected into the center of the sphere. The travel times of

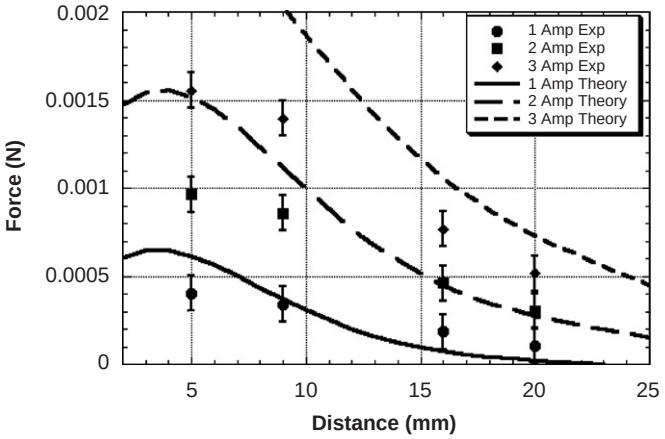

Fig. 5. Theoretical magnetic forces exerted on a ferrofluid compared to experimental values at 1, 2, and 3 A of current passing through the electromagnet.

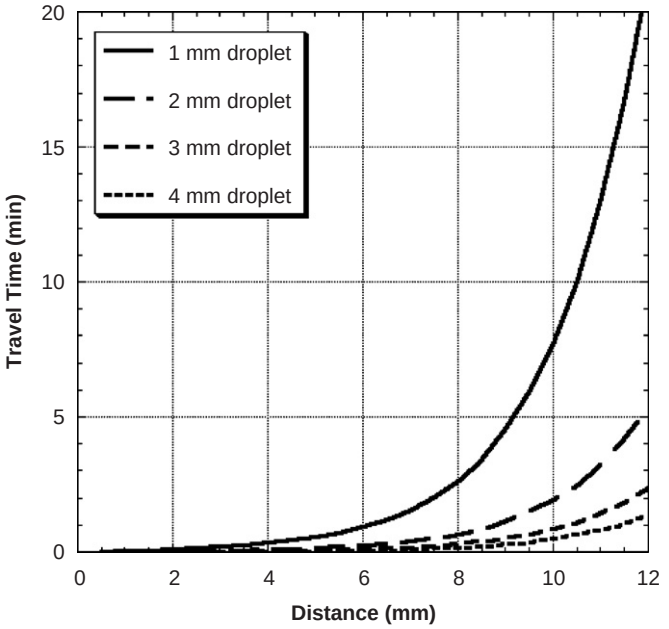

Fig. 6. Calculated travel times for different diameter droplets through a aqueous medium with a viscosity of 50 Pa s to a 5 mm thick by 5×20 mm bar magnet containing 80 wt% NdFeB powder with the magnetic field through the thickness.

Table 1
Theoretical vs. experimental travel times for different droplet sizes

Diameter of droplet (mm)	Travel distance (mm)	Theoretical time (min)	Experimental time (min)
1.0	12	21.2	15.0
1.8	12	6.6	4.0
2.0	11	3.2	2.5

the droplets were compared to the numerical calculations (Table 1). Higher velocities of larger droplets were clearly demonstrated. Although the calculated and measured travel times were within reasonable agreement, the measured times were consistently somewhat shorter than those estimated by the theoretical model. The most likely reason for this systematic difference is the assumption that the droplet acts as a magnetic dipole located at the center of the droplet. Due to the field gradients in the system, the effective position of the dipole will be displaced towards the magnet and hence the resulting magnetic forces will be larger than those predicted by the current model.

Several interesting effects were observed in the images captured by the time-lapse photography that have not yet been considered in the calculations. At larger droplet sizes, the droplet shape deforms from a sphere to a teardrop as it moves through the viscous medium toward the magnet. In addition, as the droplet accelerates towards the magnet, separation of the tail of the teardrop was sometimes observed. This resulted in smaller droplets, which require longer travel times to the permanent magnet.

4. Conclusions

While the droplets may change shape and break up, the numerical method for estimating the travel times is sufficiently accurate to provide an upper bound to the travel time. The calculated forces imposed on the droplets by small magnets predict that travel times of seconds to minutes should be possible in a clinical environment. Moreover, the numerical method can be utilized as an aid for the future design of magnets with appropriate sizes and strengths. All of these results show promise for the proposed treatment of retinal detachment.

More advanced modeling will be required to integrate the forces over the total volume of the particle and to investigate the deformation of larger droplets. Both variation of forces within the droplet and hydrodynamic shear stress from the viscous medium may contribute to deformation of the droplet. The portion of the droplet closest to the magnet experiences a greater force than the section further away. This difference is likely a factor contributing to droplet shape change. Continuing work will include investigations of the shear thinning behavior of the droplet as it accelerates, as well as variance in the magnetic forces within the droplet.

Acknowledgements

The authors are grateful for the financial support of the Orris C. and Beatrice Dewey Hirtzel Memorial Foundation, the NSF Materials World Network (DMR-0602932) for the Study of Macromolecular Ferrofluids, the National Eye Institute of the NIH under SBIR contract B6867G1, and the ARC Discovery Grant—DP0559333.

References

[1] J.P. Dailey, J.P. Phillips, C. Li, et al., J. Magn. Magn. Mater. 194 (1999) 140.
[2] M. Rutnakornpituk, V.V. Baranauskas, J.S. Riffle, et al., Eur. Cells Mater. 3 (2002) 102.
[3] J.P. Stevenson, M. Rutnakornpituk, M.L. Vadala, et al., J. Magn. Magn. Mater. 225 (2001) 47.
[4] M.L. Vadala, M.A. Zalich, D.B. Fulks, et al., J. Magn. Magn. Mater. 293 (2005) 162.
[5] K.S. Wilson, J.D. Goff, J.S. Riffle, et al., Polym. Adv. Technol. 16 (2005) 200.
[6] M.A. Martenyuk, Y.L. Raikher, M.I. Shlionmis, Sov. Phys. JETP 38 (1974) 413.
[7] M.I. Shlionmis, Sov. Phys. JETP 34 (1972) 1291.
[8] M.I. Shlionmis, Soviet Phys. Uspekhi 17 (1974) 153.
[9] M.I. Shlionmis, Phys. Rev. E 64 (2001) 063501.
[10] M.I. Shlionmis, Phys. Rev. E 64 (2001) 060501.
[11] M.I. Shlionmis, Ferrohydrodynamics: Retrospective and Issues, Springer, Berlin, 2002.
[12] B.U. Felderhof, Phys. Rev. E 62 (2000) 3848.
[13] B.U. Felderhof, Phys. Rev. E 64 (2001) 063502.
[14] B.U. Felderhof, H.J. Kroh, J. Chem. Phys. 110 (1999) 7403.
[15] W. He, S.J. Lee, D.C. Jiles, et al., J. Appl. Phys. 10 (2003) 7459.
[16] V. Bashtovoi, G. Bossis, P. Kuzhir, et al., J. Magn. Magn. Mater. 289 (2005) 376.

[17] J.G. Veguera, Y.I. Dikansky, J. Magn. Magn. Mater. 289 (2005) 87.
[18] V.A. Naletova, V.A. Turkov, V.V. Sokolov, et al., J. Magn. Magn. Mater. 289 (2005) 367.
[19] V.A. Naletova, V.A. Turkov, A.N. Tyatyuskin, J. Magn. Magn. Mater. 289 (2005) 370.
[20] C. Rinaldi, A. Chaves, S. Elborai, et al., Curr. Opin. Coll. Interface Sci. 10 (2005) 141.
[21] T.H. Boyer, Am. J. Phys. 56 (1988) 688.